

Inertia - gravity wave generation by the tropospheric mid-latitude jet as given by the FASTEX radiosoundings

R. Plougonven*, H. Teitelbaum and V. Zeitlin

Laboratoire de Météorologie Dynamique, Paris, France.

1. Introduction

Jets and fronts are known to be important sources of inertia-gravity waves (IGW) (e.g. Fritts and Nastrom (1992)) but the generation mechanisms involved are not yet well understood. Geostrophic adjustment due to the evolution of the large-scale flow is one mechanism that has been emphasized by several studies, both observational (Uccellini and Koch (1987)) and numerical (O'Sullivan and Dunkerton (1995); Zhang et al. (2001)), particularly in the exit region of jets. Recent observational studies of inertia-gravity waves in the vicinity of the mid-latitude jet when the latter is distorted, with the upper-tropospheric geopotential exhibiting a deep trough, (Thomas et al. (1999); Pavelin et al. (2001); Hertzog et al. (2001)) have referred to the numerical simulations of O'Sullivan and Dunkerton (1995) to suggest that geostrophic adjustment was the dynamical mechanism generating the waves.

We have used a sample of 224 radiosoundings obtained from the FASTEX campaign to study how gravity wave activity varied in the vicinity of the midlatitude jet, and to identify regions that are most favorable to inertia-gravity wave generation (Plougonven et al. (2003)). The soundings chosen were launched in the Atlantic Ocean, far from orographic sources of gravity waves. The intensity of the gravity waves in the soundings was studied as a function of the distance to the jet: the most intense gravity wave activity was found near the jet, confirming that the jet region was the dominant source of gravity waves. Further examination revealed that two specific regions were particularly favorable to intense gravity wave activity: the vicinity of the maxima of the velocity and regions where the jet is highly curved, in the troughs.

We present below a detailed case study of a large-scale IGW observed in the lower stratosphere in such a region in a trough, and show that geostrophic adjustment is the likely source mechanism at the origin of the wave.

2. Configuration of the large-scale flow on February 5 and 6, 1997

Analyses from the European Center for Medium-Range Weather Forecast (ECMWF) are used to describe the flow on a large-scale. On February 5 and 6, 1997, a deep trough can be seen in the upper-tropospheric geopotential. Correspondingly, the jet is severely distorted toward the South, as can be seen in figure 1. The trough propagates over the Atlantic ocean in approximately 2 days, and it progressively becomes narrower.

The analyses from the ECMWF also allow us to obtain indications on regions where imbalance may be forced by the large-scale evolution of the flow. The cross-stream Lagrangian Rossby number

$$Ro_{\perp} = \frac{|\mathbf{v}_{ag}^{\perp}|}{|\mathbf{v}|}, \quad (1)$$

where \mathbf{v}_{ag}^{\perp} is the part of the ageostrophic velocity that is normal to the flow, has been proposed by Koch and Dorian (1988) as an indicator of the imbalance due to the large-scale flow. Its relevance has recently been confirmed in numerical simulations by Zhang et al. (2000).

The maxima of Ro_{\perp} are shown in figure 1, superimposed on the wind and isotachs. The large-scale evolution of the flow forces a region of imbalance deep in the trough, where the wind has a strong curvature. The isotachs show that the regions of imbalance are actually associated to the exit region of the south-eastward jet streak and the entry region of the north-eastward jet streak.

3. Generation of IGW from the jet by geostrophic adjustment as seen from the radiosoundings

As part of the FASTEX database, five soundings are available on February 5 and 6 near the region of imbalance indicated by the ECMWF.

Radiosoundings 1 and 2 were located just downstream of the trough, in the entry region of the north-eastward jet. They were launched on February 5, respectively at 11.30GMT and 20.31GMT. The location of sounding 2

* *Corresponding author address:* Riwal Plougonven, National Center for Atmospheric Research, P.O. Box 3000, Boulder, CO 80307. Email: riwal.plougonven@polytechnique.org

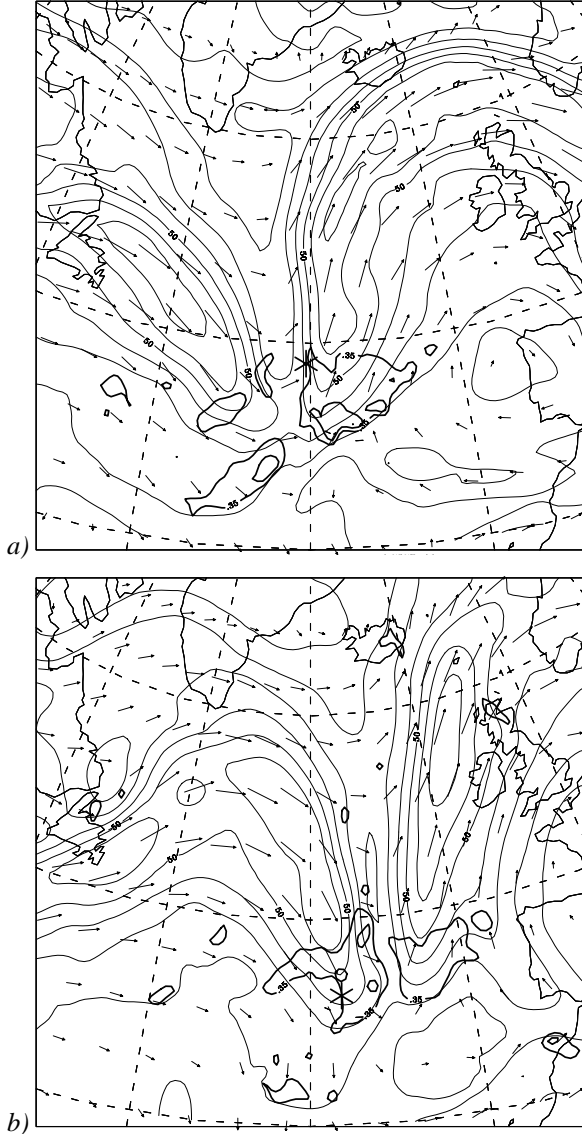


Figure 1: Maps of the wind velocity (arrows) and norm (contours every $10ms^{-1}$) for February 6, 00GMT and 18GMT, at log-pressure height $Z = 8km$, obtained from analyses of the ECMWF. The thick contours indicate the maxima of the cross-stream Lagrangian Rossby number (contours every 0.2, starting at 0.35), plotted only in regions where the wind exceeds $20ms^{-1}$. The stars indicate the location of soundings 2 and 3 (upper-panel) and sounding 4 and 5 (lower-panel).

is indicated in figure 1a). Sounding 3 was launched from approximately the same location as the preceding, but on February 6, at 5.36GMT. The trough had propagated to the East and hence radiosounding 2 was in the region of weak winds between the two branches of the jet (see figure 1). These three first radiosoundings were located on the border or just downstream of the imbalance associated to the entry region of the north-eastward jet streak. They have a resolution of about $50m$.

The last two soundings were launched from the Azores Islands, on February 6, at 17.19GMT and 23.24GMT respectively, and have a lower resolution ($\sim 300m$). As can be seen from figure 1b), they were located in the region of imbalance, in the exit region of the south-eastward jet-streak.

The velocity profiles of the five radiosoundings were processed in the following way to separate a background and a perturbation wind profile: the observed profiles were first interpolated using a cubic spline. A high-pass non-recursive filter was then applied to suppress perturbations with scales larger than $5km$. Details regarding the filter and its transfer function may be found in Scavuzzo et al. (1998).

In the five radiosoundings, a clear and intense IGW can be seen in the lower stratosphere (see fig. 2 and 3) with energy propagating upwards (anticyclonic rotation in the hodographs, fig. 4). In radiosoundings 1, 3, 4 and 5, indications of an IGW propagating downward in the troposphere are also present. In sounding 5, the downward propagating wave is particularly clear (fig. 3). As expected, its amplitude ($4ms^{-1}$) is smaller than that of the stratospheric wave ($7ms^{-1}$). These tropospheric IGWs propagating energy downward suggest that the waves are generated at the level of the jet.

The characteristics of the waves (see table 1) were obtained using the hodograph method, after an additional filtering of the velocity profiles (the filtering window used was typically $1.5 - 4km$ and, by removing smaller scale perturbations, allowed to isolate the waves of interest).

Knowing the aspect ratio R of the ellipse in the hodograph, and the vertical wavelength λ_z of a given quasi-monochromatic wave are known, we estimate the intrinsic frequency as $\omega = f/R$, and the horizontal wavelength λ_H using the linear dispersion relation for hydrostatic waves:

$$\omega^2 = f^2 + \frac{N^2 \lambda_z^2}{\lambda_H^2}. \quad (2)$$

Temperature measurements give a Brunt-Vaisala frequency of $2.1 \cdot 10^{-2}s^{-1}$ in the lower stratosphere.

The characteristics of the waves observed in the lower stratosphere are nearly identical for the first three radiosoundings, hence we consider that it is the same wave.

#	Height	λ_z	R	$ u'_{max} $
1	10.5 – 14.5km	2.2km	0.7	8ms ⁻¹
2	10.5 – 15km	2.2km	0.7-0.9	9ms ⁻¹
3	9 – 15.5km	2.1km	0.7	7ms ⁻¹
4	9.5 – 15km	2.4km	0.35	7ms ⁻¹
5t	1 – 5km	2.3km	0.5	4ms ⁻¹
5s	9 – 14km	2.5km	0.5 – 0.65	7ms ⁻¹

Table 1: Characteristics of the waves observed in the lower stratosphere in radiosoundings 1-5, on February 5-6: the columns contain, successively, the radiosounding number, the height range in which the wave is detected, the vertical wavelength, the aspect ratio, and the order of magnitude of the maximum wave velocity. Two rows are present for sounding 5: one for the tropospheric wave (5t), and one for the stratospheric wave (5s).

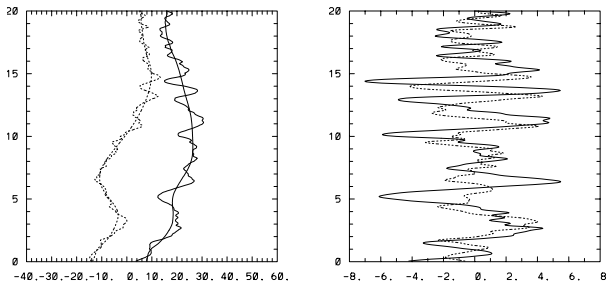


Figure 2: Profiles for the total and background wind (left) and for the perturbation wind (right) for sounding 3; plain line for the zonal velocity, dashed line for the meridional velocity.

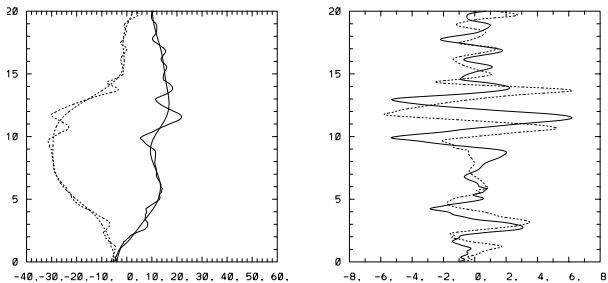


Figure 3: As in fig. 2, for sounding 5. An IGW with energy propagating upward is apparent in the lower stratosphere, and an IGW with energy propagating downward can also be seen in the troposphere.

Taking the aspect ratio to be 0.7 we estimate the intrinsic period and the horizontal wavelength as ~ 12 hours and $400 - 450$ km, respectively.

The lower stratospheric wave in the last two soundings have comparable characteristics, although the aspect ratios are smaller, particularly for sounding 4. This could be due to the strong vertical shear in the background wind present in that sounding. The estimated intrinsic period and horizontal wavelength are of approximately 6 hours and 200 km for sounding 4, and 10-12 hours and $330 - 500$ km for sounding 5. These last values are consistent with the ones found for the first three radiosoundings.

The orientation of the wave vector can be determined from that of the major axis of the hodographs' ellipse, and its direction from the profiles of potential temperature. This analysis shows the wave vector pointing to North-West in the first two radiosoundings, and pointing to West-North-West in the third radiosounding (see fig. 4). Hence, the wave-vector in the radiosoundings 1 and 2 is transverse to the mean-flow.

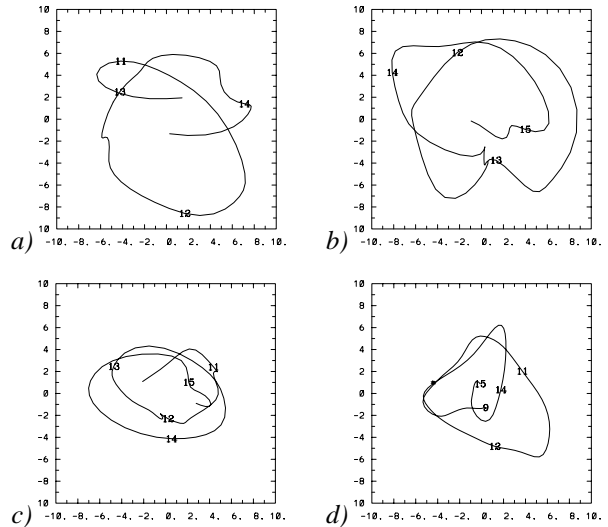


Figure 4: Hodographs of the wind perturbation for soundings 1 (panel a), 2 (b), 3 (c) and 5 (d). The numbers indicate the height in km. An additional filtering of scales smaller than 300 m was applied in a) and b).

Maps of the divergence of the horizontal wind were also obtained from the ECMWF analyses. They exhibit patterns of alternating convergence and divergence, interpreted as a signature of a large-scale IGW, in the location of the soundings presented here, and with comparable orientation. This brings further support to our interpretation of the soundings.

4. Summary and discussion

We have analysed a wave present in the lower stratosphere (10 – 15km) in five radiosoundings launched during the FASTEX campaign, on February 5 and 6, 1997. The times of the radiosoundings cover 36 hours, but all five are located similarly relative to the large-scale flow, *i.e.* in a deep trough, where the jet decelerates and veers from a south-eastward to a north-eastward orientation.

Maps of the cross-stream Lagrangian Rossby number were obtained from the analyses of the ECMWF in order to diagnose regions of imbalance forced by the evolution of the large-scale flow. These maps showed that imbalance was systematically present in the deepest part of the trough, associated with the exit region of one branch of the jet and the entry region of the other. All five radiosoundings were located in, or just downstream of, these regions of imbalance.

In all five radiosoundings, an intense ($7 - 9\text{ms}^{-1}$) IGW was observed in the lower stratosphere. In several of the radiosoundings, and particularly in sounding 5, an IGW with the same vertical wavelength and comparable aspect ratio could be seen in the troposphere with energy propagating downward, providing strong indications that the waves observed in the lower stratosphere were generated at the level of the jet, in the upper-troposphere.

The characteristics of the lower stratospheric IGW were obtained using the hodograph method, and showed that it is the same wave that is observed in the first three soundings. It has a vertical wavelength of 2.2km, and its intrinsic frequency and horizontal wavelength are estimated as $1.4f$ and 400 – 450km respectively. The characteristics of the lower stratospheric wave in the last two radiosoundings are also comparable.

These elements support the interpretation of these soundings as revealing one intense, large-scale, low-frequency IGW being generated by geostrophic adjustment due to the large-scale dynamics of the jet. The maps of Ro_{\perp} and the observation of an tropospheric IGW propagating energy downward, particularly in the last sounding, are strong indications that the large-scale flow, in this configuration, is continuously forcing large-scale IGWs.

Other similar configurations of the flow during the month of February were investigated in the same way. The available soundings, although less numerous, showed comparable IGWs in the lower stratosphere, and in some cases in the troposphere, with energy propagating downward, suggesting that the forcing of IGW by geostrophic adjustment could be systematic in this configuration of the flow.

These observations are generally in agreement with the numerical simulations of O’Sullivan and Dunkerton (1995), but differences need to be pointed out: first, the generation region in our case is located deeper in the

trough of geopotential, which is consistent with the results of Hertzog et al. (2001). Second, the soundings analysed contained IGW not only propagating upward from the jet, but also, with similar characteristics, propagating downward in the troposphere, as in the observations of Thomas et al. (1999).

REFERENCES

- Fritts, D. and G. Nastrom, 1992: Sources of mesoscale variability of gravity waves. Part II: Frontal, convective, and jet stream excitation. *J. Atmos. Sci.*, **49**, 111–127.
- Hertzog, A., C. Souprayen, and A. Hauchecorne, 2001: Observation and backward trajectory of an inertia-gravity wave in the lower stratosphere. *Annales Geophysicae*, **19**, 1141–1155.
- Koch, S. E. and P. B. Dorian, 1988: A mesoscale gravity wave event observed during CCOPE. Part III: wave environment and possible source mechanisms. *Mon. Wea. Rev.*, **116**, 2570–2591.
- O’Sullivan, D. and T. Dunkerton, 1995: Generation of inertia-gravity waves in a simulated life cycle of baroclinic instability. *J. Atmos. Sci.*, **52**, 3695–3716.
- Pavelin, E., J. Whiteway, and G. Vaughan, 2001: Observation of gravity wave generation and breaking in the lowermost stratosphere. *J. Geophys. Res.*, **106**, 5173–5179.
- Plougonven, R., H. Teitelbaum, and V. Zeitlin, 2003: Inertia-gravity wave generation by the tropospheric mid-latitude jet as given by the fastex radiosoundings. *submitted to J. Geophys. Res.*
- Scavuzzo, C., M. Lamfri, H. Teitelbaum, and F. Lott, 1998: A study of the low-frequency inertio-gravity waves observed during the Pyrénées experiment. *J. Geophys. Res.*, **103**, 1747–1758.
- Thomas, L., R. Worthington, and A. McDonald, 1999: Inertia-gravity waves in the troposphere and lower stratosphere associated with a jet stream exit region. *Ann. Geophysicae*, **17**.
- Uccellini, L. and S. Koch, 1987: The synoptic setting and possible energy sources for mesoscale wave disturbances. *Mon. Wea. Rev.*, **115**, 721–729.
- Zhang, F., S. Koch, C. Davis, and M. Kaplan, 2000: A survey of unbalanced flow diagnostics and their application. *Adv. Atmos. Sci.*, **17**, 165–183.
- 2001: Wavelet analysis and the governing dynamics of a large amplitude mesoscale gravity wave event along the east coast of the united states. *Q.J.R. Meteorol. Soc.*, **127**, 2209–2245.